


Article

The English (H6R) Mutation of the Alzheimer's Disease Amyloid- β Peptide Modulates Its Zinc-Induced Aggregation

Sergey P. Radko^{1,2,*}, Svetlana A. Khmeleva², Dmitry N. Kaluzhny¹, Olga I. Kechko¹, Yana Y. Kiseleva³, Sergey A. Kozin¹, Vladimir A. Mitkevich¹  and Alexander A. Makarov¹

¹ Engelhardt Institute of Molecular Biology, Russian Academy of Sciences, 119991 Moscow, Russia; uzhny@mail.ru (D.N.K.); olga.kechko@gmail.com (O.I.K.); kozinsa@gmail.com (S.A.K.); mitkevich@gmail.com (V.A.M.); aamakarov@eimb.ru (A.A.M.)

² Institute of Biomedical Chemistry, 119121 Moscow, Russia; diny1204@yandex.ru

³ Russian Scientific Center of Roentgenoradiology, 117485 Moscow, Russia; yana.kiseleva@gmail.com

* Correspondence: radkos@yandex.ru

Received: 4 June 2020; Accepted: 24 June 2020; Published: 25 June 2020



Abstract: The coordination of zinc ions by histidine residues of amyloid-beta peptide ($A\beta$) plays a critical role in the zinc-induced $A\beta$ aggregation implicated in Alzheimer's disease (AD) pathogenesis. The histidine to arginine substitution at position 6 of the $A\beta$ sequence (H6R, English mutation) leads to an early onset of AD. Herein, we studied the effects of zinc ions on the aggregation of the $A\beta$ 42 peptide and its isoform carrying the H6R mutation (H6R- $A\beta$ 42) by circular dichroism spectroscopy, dynamic light scattering, turbidimetric and sedimentation methods, and bis-ANS and thioflavin T fluorescence assays. Zinc ions triggered the occurrence of amorphous aggregates for both $A\beta$ 42 and H6R- $A\beta$ 42 peptides but with distinct optical properties. The structural difference of the formed $A\beta$ 42 and H6R- $A\beta$ 42 zinc-induced amorphous aggregates was also supported by the results of the bis-ANS assay. Moreover, while the $A\beta$ 42 peptide demonstrated an increase in the random coil and β -sheet content upon complexing with zinc ions, the H6R- $A\beta$ 42 peptide showed no appreciable structural changes under the same conditions. These observations were ascribed to the impact of H6R mutation on a mode of zinc/peptide binding. The presented findings further advance the understanding of the pathological role of the H6R mutation and the role of H6 residue in the zinc-induced $A\beta$ aggregation.

Keywords: amyloid- β ; English mutation; zinc; aggregation

1. Introduction

The aggregation of amyloid- β peptide ($A\beta$) is considered as a crucial event in pathogenesis of Alzheimer's disease (AD)—a devastating neurodegenerative disorder which affects tens of millions of people throughout the world [1]. Though molecular mechanisms underlying $A\beta$ aggregation were a subject of intensive in vitro and in vivo studies for about three decades, they are still incompletely understood [2,3]. Among factors which can potentially contribute to the in vivo $A\beta$ aggregation, zinc ions (Zn^{2+}) have attracted a constant interest [4,5] ever since they were found to trigger rapid $A\beta$ aggregation in vitro [6]. It is worth noting that amyloid plaques (the deposits in brain parenchyma, primarily composed of 40- and 42-amino-acid-long $A\beta$ peptides— $A\beta$ 40 and $A\beta$ 42, correspondingly), which are a hallmark of AD [7], are abnormally loaded with zinc [8,9]. Being an important neuromodulator, zinc, when released from synaptic vesicles during neuronal excitation, can be transiently present in a synaptic cleft at considerably high concentrations—up to 300 μ M [10]. Interestingly, the transgenic AD model mice with a knocked-out gene coding for the specific zinc transporter Zn-T3 (responsible for pumping zinc into synaptic vesicles) do not develop amyloid

plaques [11]. The plausible role of zinc in AD pathogenesis as a causative agent alongside that of another vital metal such as copper has inspired a development of the approach known as “AD chelation therapy” [12], as a part of efforts to find a cure for the disease.

It is known that Zn^{2+} triggers the formation of $A\beta$ aggregates which lack the defined cross- β -sheet organization typical for $A\beta$ fibrils and are often referred to as “amorphous” aggregates [10]. The Zn^{2+} -induced $A\beta$ aggregation is undoubtedly initiated by a formation of Zn^{2+} - $A\beta$ complexes: $A\beta$ peptides bind zinc via the Zn^{2+} coordination involving histidine residues H6, H13, and H14 of the peptide’s N-terminal region consisting of amino acid residues 1–16 and referred to as a metal-binding domain (MBD) [10,13]. Due to the importance of histidine residues for the Zn^{2+} coordination, their role in the Zn^{2+} -dependent $A\beta$ aggregation has been probed in a number of studies, using various substitutions for histidine residues in truncated and full-length $A\beta$ peptides ($A\beta_{28}$, $A\beta_{40}$, and $A\beta_{42}$) [14–16]. The substitution of alanine residue for either H13 or H14, but not H6, was demonstrated to suppress the effect of Zn^{2+} on the fibrillar aggregation of these peptides [15,16]. The double substitution—R5 and H6 with alanine residues—was also found to have no impact on the Zn^{2+} -triggered “coil-to- β -sheet” conformational transition in $A\beta_{28}$ and $A\beta_{40}$ peptides [15]. However, as we have earlier shown, the substitution of H6 with arginine residue (H6R, known as the “English mutation” associated with the early onset of AD [17]), while not preventing the Zn^{2+} -induced $A\beta_{42}$ aggregation, resulted nonetheless in some reduction of the number of sedimentation-prone Zn^{2+} -induced aggregates (at Zn^{2+} /peptide ratios of 1 to 3), compared to the wild-type $A\beta_{42}$ [18]. $A\beta_{42}$ peptides bearing the H6R mutation (H6R- $A\beta_{42}$) were also shown to produce Zn^{2+} -induced aggregates of a smaller size at a Zn^{2+} /peptide ratio below 1 [19]. Still, many aspects of how the H6R mutation can affect the Zn^{2+} -induced aggregation of full-length $A\beta$ peptides are unclear yet.

The aim of the present work was to get further insights into the effects of H6R substitution on the *in vitro* aggregation of the $A\beta_{42}$ peptide, triggered by Zn^{2+} . To achieve this aim, the Zn^{2+} -induced aggregation of synthetic $A\beta_{42}$ and H6R- $A\beta_{42}$ peptides in the presence of various amount of Zn^{2+} was studied with circular dichroism spectroscopy (CD), dynamic light scattering (DLS), turbidimetric and sedimentation methods, and fluorescence assays utilizing bis-ANS and thioflavin T fluorescent dyes. The $A\beta_{42}$ and H6R- $A\beta_{42}$ peptides were found to attain different conformations in Zn^{2+} -induced amorphous aggregates upon complexing with Zn^{2+} that leads to a formation of aggregates with distinct characteristics.

2. Materials and Methods

2.1. Materials

Synthetic peptides $A\beta_{42}$ (DAEFRHDSGYEVHHQKLVFFAEDVGSNKGAIIGLMVGGVVIA) and H6R- $A\beta_{42}$ (purity > 95%) were purchased as a lyophilized solid from Biopeptide Co., LLC (San Diego, CA, USA). The $A\beta_{42}$ sequence is presented in the parenthesis. The residue marked in bold is substituted in the H6R- $A\beta_{42}$ isoform with the arginine residue. All chemicals used were obtained from Sigma-Aldrich (St. Louis, MO, USA) and were of an analytical grade or higher. Chloride of zinc served as a source of zinc ions. The Milli-Q quality water was used to prepare all solutions; Milli-Q water and stock buffer solutions were filtered through a 0.22 μ m pore syringe filter (Merck, Kenilworth, NJ, USA, #SLGP033RB).

2.2. Peptide Solutions and Preparation of Zinc-Induced $A\beta_{42}$ Aggregates

To prepare $A\beta_{42}$ solutions, $A\beta_{42}$ peptides were treated with hexafluoroisopropanol (HFIP), dried, and dissolved in 10 mM NaOH at a concentration of 0.5 mM. The $A\beta_{42}$ solutions in 10 mM NaOH were adjusted with 100 mM HEPES-buffer (pH 5.0) to pH 6.8 and subjected to centrifugation (30 min, 16,000 \times g, 4 $^{\circ}$ C) to remove insoluble peptide aggregates. Peptides in the supernatant were quantified spectrophotometrically (based on the molar extinction coefficient $\epsilon_{280} = 1490 \text{ M}^{-1} \times \text{cm}^{-1}$ [20]) and diluted with appropriate buffers to provide $A\beta_{42}$ solutions of desired concentrations in the buffer

containing 10 mM HEPES (pH 6.8) and 50 mM NaCl (further referred to as 'buffer H'). The peptide solutions were kept on ice until further use. H6R-A β 42 peptide solutions were prepared in an identical manner.

The Zn²⁺-induced A β aggregation was triggered by mixing aliquots of 40- μ M peptide solutions with buffer H supplemented with ZnCl₂ at various concentrations. The mixtures were incubated under quiescent conditions at room temperature for 30 min. For bis-ANS (4,4'-dianilino-1,1'-binaphthyl-5,5'-disulfonic acid)-based fluorescence measurements, an aliquot of the stock bis-ANS solution (700 μ M in buffer H) was added to the peptide solution at the peptide/bis-ANS molar ratio of 10:1 prior to inducing peptide aggregation. The final peptide concentration in all cases was 25 μ M.

2.3. Circular Dichroism Spectroscopy

CD spectra of A β 42 and H2R-A β 42 peptides were acquired using a J-715 spectropolarimeter (JASCO, Easton, MD, USA). A 25- μ M solution of A β peptides either in a monomeric or aggregated state in buffer H was placed into a quartz cell with a path length of 1 mm, and CD spectra were collected from 195 to 260 nm with a 1 nm interval at 25 °C. Every CD spectrum was an average of three separate measurements. The A β aggregation was induced 20 min prior to a measurement by adding Zn²⁺ to the A β solutions at Zn²⁺/A β molar ratios of 2 and 4. The analysis of the peptides' secondary structure was carried out using software package CDNN [21,22].

2.4. Turbidimetry and Dynamic Light Scattering

The Zn²⁺-induced aggregation of A β 42 and H6R-A β 42 peptides was evaluated by measuring optical density of A β preparations at 405 nm (OD₄₀₅) on an Agilent 8453E spectrophotometer (Agilent Technologies, Santa Clara, CA, USA). The OD₄₀₅ values measured in the absence of Zn²⁺ were taken as the initial (zero time) values.

DLS measurements were carried out on a Zetasizer Nano ZS apparatus (Malvern Instruments Ltd., Malvern, UK) at 25 °C as described elsewhere [18,23]. The apparatus is able to measure particles sizes in the range of 0.6 nm to 10 μ m. The characteristic size of A β aggregates was expressed in terms of an average "diameter", since instrument software approximates the heterogeneous population of A β aggregates by a population of spherical particles with the identical distribution of a diffusion coefficient. The number particle distribution was used by the instrument software to calculate average particle diameters.

2.5. Sedimentation Assay

A β preparations with and without added Zn²⁺ were subjected to centrifugation (16,000 \times g, 10 min, 20 °C). Supernatants were sampled and peptide concentrations were determined with a commercial BCA assay (Thermo Fisher Scientific, Waltham, MA, USA, #23235). The relative amount of peptides in the supernatant was calculated as C/C_0 , where C and C_0 are peptide concentrations in the supernatant in the presence and absence of Zn²⁺, respectively.

2.6. Fluorimetry

Fluorescence measurements were carried out on an Infinite M200 PRO microplate reader (TECAN, Männedorf, Switzerland) using Corning 96-well microplates. For bis-ANS fluorescence measurements, aliquots of bis-ANS containing A β preparations were placed into wells in triplicates and aggregation was initiated by the addition of Zn²⁺-containing buffer H. The final volume of each sample was 100 μ L. After the 30-min incubation, fluorescence was recorded using 400 and 500 nm wavelengths for excitation and emission, respectively. The fluorescence was corrected by subtracting values of fluorescence in wells with merely bis-ANS in buffer H to provide the "pure" bis-ANS fluorescence of bis-ANS/A β complexes, F . To perform thioflavin T (4-(3,6-dimethyl-1,3-benzothiazol-3-ium-2-yl)-N,N-dimethylaniline chloride, ThT)-based fluorescence measurements, A β preparations were mixed with aliquots of the ThT solution in buffer H so as to provide the final A β and ThT concentrations of 25 μ M each. The aliquots of

A β /ThT mixtures were placed in wells in triplicates and the Zn²⁺-induced aggregation was initiated as above. The ThT fluorescence was measured as described above, except for excitation and emission wavelengths which were correspondingly set at 450 and 482 nm.

3. Results

3.1. The Zn²⁺-Induced Aggregation of A β 42 and H6R-A β 42 Peptides Measured with Turbidity, DLS, and Sedimentation Methods

The addition of Zn²⁺ to solutions of A β 42 and its mutated isoform, H6R-A β 42, triggered a rapid peptide aggregation manifested by a rise in solution turbidity (Figure 1). Turbidity values appeared to approach a plateau by 30 min of incubation for all Zn²⁺/peptide molar ratios tested. The OD₄₀₅ values measured at 30-th min of incubation were flattened out at the Zn²⁺/peptide ratios of 2 and above, showing considerably higher turbidity for the mutant peptide, compared to the intact (the insert in Figure 1A). The sizes of A β 42 and H6R-A β 42 aggregates measured by DLS after 30-min incubation were indistinguishable within the experimental scatter and equal to 1.5–2 μ m in diameter for both peptides at Zn²⁺/peptide ratios of 1 to 4 (Figure 2). In the absence of Zn²⁺, the species with a characteristic size of about 14–17 nm were detected by DLS in the A β 42 and H6R-A β 42 solutions within the 30-min incubation interval that may be attributed to the presence of low molecular weight A β 42 oligomers [24]. Since at Zn²⁺/peptide molar ratios of 2 to 4, the size of A β aggregates was similar for both isoforms (Figure 2) while turbidity values significantly differed (Figure 1), we tested by the sedimentation method whether the number of peptides involved in the formation of Zn²⁺-induced aggregates varied for A β 42 and H6R-A β 42 isoforms. At the Zn²⁺/peptide molar ratio of 4, the fraction of A β 42 and H6R-A β 42 peptides included into sedimentation-prone Zn²⁺-induced aggregates was found to equal (0.91 \pm 0.04) and (0.86 \pm 0.05), respectively. Thus, practically all peptides were in an aggregated state for both isoforms at that Zn²⁺/peptide ratio. Consequently, at least at the highest Zn²⁺/peptide ratio used, the observed differences in turbidity of A β 42 and H6R-A β 42 preparations (Figure 1) could be accounted for by neither the aggregate size (which is similar, Figure 2) nor the number of aggregated peptides.

3.2. Effect of the H6R Mutation on Zn²⁺-Induced Conformational Changes in A β Peptides

In the absence of Zn²⁺, CD spectra for A β 42 and H6R-A β 42 peptides were found to slightly differ (Figure 3A,B). Deconvolution of the CD spectra revealed that the native A β 42 peptide possessed predominantly an α -helix/random coil secondary structure (Figure 3C). Such structural organization was observed for HFIP-treated A β peptides dissolved in aqueous solutions and ascribed to their monomeric state [25,26]. For the mutant peptide, H6R-A β 42, the random coil organization dominated, and an increase in β -sheet structure, compared with the intact peptide, was noticeable (Figure 3D). This observation agreed with the molecular dynamic simulation results on structural characteristics of A β 42 and H6R-A β 42 peptides [27]. A higher β -structure content in A β peptides was suggested to promote their self-aggregation [28,29] and may have been responsible for the known higher self-aggregation propensity of the H6R-A β mutants compared with the intact A β peptides [30,31]. Upon addition of Zn²⁺, the CD spectrum changed for the A β 42 peptide, while no changes were observed practically for H6R-A β 42 (Figure 3A,B). Consequently, for H6R-A β 42, the Zn²⁺-induced aggregation was not accompanied by sufficient alterations in peptide structure (Figure 3C). At the same time, the intact peptide underwent a structural reorganization manifested by a steady increase in random coil and β -sheet content with Zn²⁺ concentration (Figure 3D). The Zn²⁺-triggered increase in β -sheet content was previously reported for the A β 42 peptide [32,33]. Interestingly, another divalent metal, copper, also known to trigger the rapid A β aggregation, was shown to induce a similar transition from the α -helix to random coil and β -sheet conformations in the A β 40 peptide [34]. Thus, the results of CD analysis indicate that A β 42 and H6R-A β 42 peptides attain different conformations in Zn²⁺-induced amorphous aggregates upon complexing with Zn²⁺. That, in turn, may lead to a distinct structural organization of these aggregates per se.

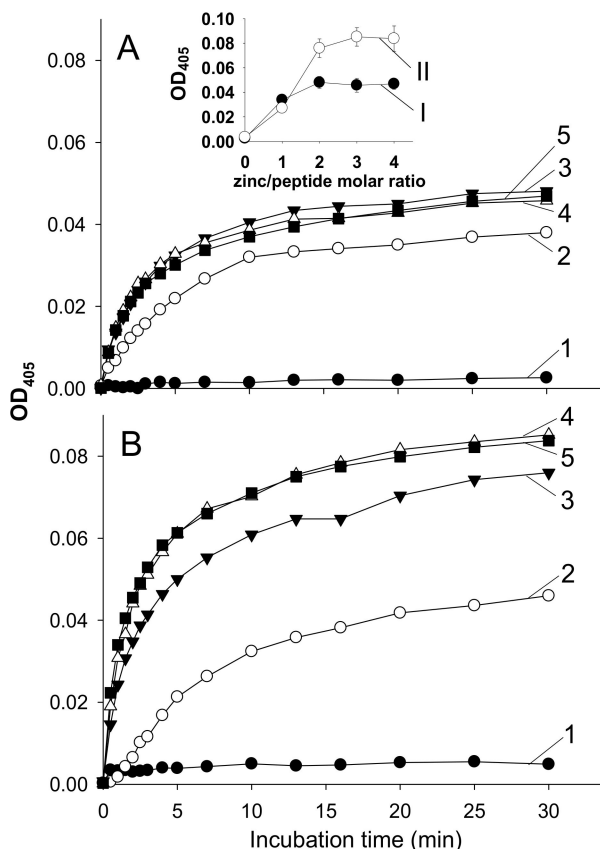


Figure 1. Dependence of turbidity (optical density at 405 nm, OD_{405}) of A β 42 and H6R-A β 42 preparations on the incubation time after the addition of Zn^{2+} at different Zn^{2+} /peptide molar ratios. Panel (A)—A β 42; panel (B)—H6R-A β 42. Curves 1, 2, 3, 4, and 5 correspond to the Zn^{2+} /peptide molar ratios of 0, 1, 2, 3, and 4, respectively. Peptides in buffer H (10 mM HEPES, pH 6.8, 50 mM NaCl); peptide concentration—25 μ M. Data points are means of three measurements; relative standard deviations for any of the points did not exceed 15%. The insert in panel (A) shows the turbidity at the 30th min of incubation as a function of the Zn^{2+} /peptide molar ratio. Curves I and II—A β 42 and H6R-A β 42 preparations, respectively.

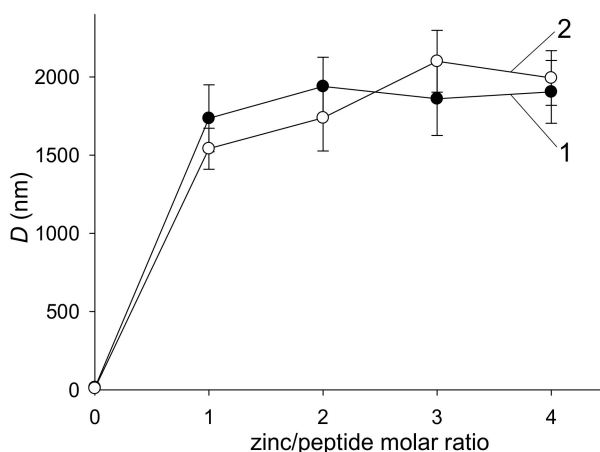


Figure 2. The characteristic diameter (D) of Zn^{2+} -induced A β aggregates, measured after 30-min incubation as a function of the Zn^{2+} /peptide molar ratio. Curves 1 and 2—A β 42 and H6R-A β 42 preparations, respectively. Peptides in buffer H (10 mM HEPES, pH 6.8, 50 mM NaCl); peptide concentration—25 μ M. The means and standard deviations for three measurements are shown.

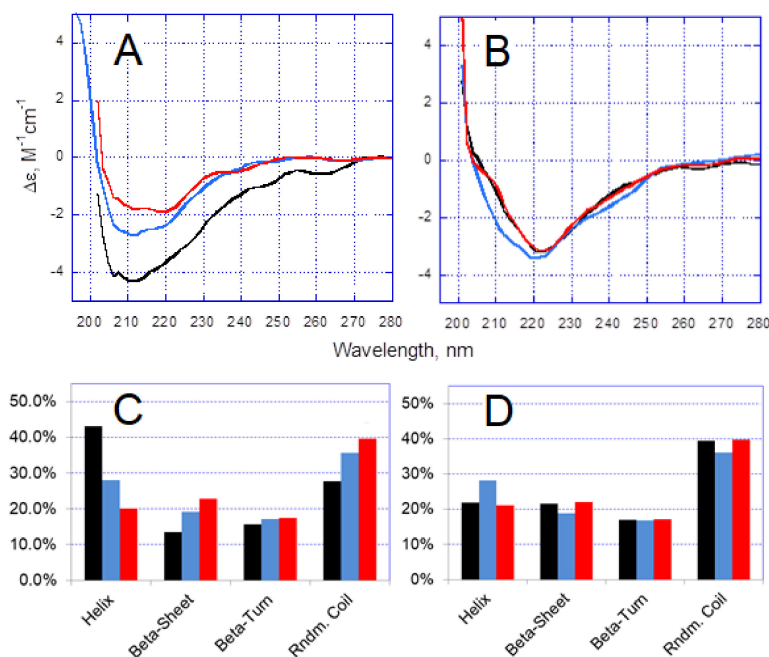


Figure 3. Circular dichroism spectra (A,B) and fractions of the secondary structure components drawn from the spectra with CDNN software (C,D). Peptides A β 42 (A,C) and H2R-A β 42 (B,D). CD spectra were collected in 20 min of incubation either in the absence or in the presence of Zn²⁺. Each CD spectrum is an average of three separate measurements. “Beta-Sheet” is a sum of parallel and antiparallel β -sheet components. The Zn²⁺ concentrations are indicated by color: Black—no Zn²⁺ added, blue and red—50 and 100 μ M Zn²⁺, respectively. Peptides in buffer H (10 mM HEPES, pH 6.8, 50 mM NaCl); peptide concentration—25 μ M.

3.3. Zn²⁺-Induced Aggregation of A β Isoforms Tested with ThT and Bis-ANS Fluorescence Assays

Since the A β 42 peptide demonstrated an increase in the β -structure content upon the addition of Zn²⁺, we tested A β 42 and H6R-A β 42 preparations with ThT (whose fluorescence is known to greatly increase upon the binding to fibrillar amyloid aggregates [35]) in order to ensure that no fibrillar A β aggregates were formed under our experimental conditions. Indeed, no appreciable differences in ThT fluorescence were observed in both the absence and presence of Zn²⁺ (Zn²⁺/peptide ratios of 1 to 4) after the 30-min incubation period for both isoforms (data not shown). Hence, one may conclude that merely amorphous A β aggregates were formed under the experimental conditions used.

As an addition to the CD analysis, we qualitatively probed the structure of Zn²⁺-induced A β 42 and H6R-A β 42 aggregates with bis-ANS—a sulfonated naphthalene derivative whose fluorescence noticeably increases in a nonpolar surrounding [36]. The dye is known to bind to proteins mostly via hydrophobic interactions and is able to report the exposure of hydrophobic clusters on protein surface as a result of a specific conformational reorganization or denaturation [36]. Bis-ANS has been employed for monitoring the Zn²⁺-induced oligomerization and aggregation of A β peptides [37–39]. Presumably, the enhancement of the dye’s fluorescence during the aggregation process is related to rearrangements in the A β conformation, triggered by the Zn²⁺ binding and the inclusion of A β into oligomers and amorphous aggregates [37,38].

The fluorescence of bis-ANS/A β complexes, F , increased with the Zn²⁺ load, reaching a plateau at the Zn²⁺/peptide ratio of 2 for both A β 42 and H6R-A β 42 isoforms (Figure 4). The F values were higher for A β 42 at the plateau than for H6R-A β 42, and the differences were statistically significant ($p < 0.05$, the two-tailed Student’s t -test). Below the Zn²⁺/peptide ratio of 2, no statistically significant differences in F values between peptides were observed ($p > 0.05$). In the absence of Zn²⁺, F values showed no appreciable changes within the 30-min incubation period for both isoforms. Hence, the results

of bis-ANS fluorescence analysis support the assumption that Zn^{2+} -induced A β 42 and H6R-A β 42 aggregates are structurally different.

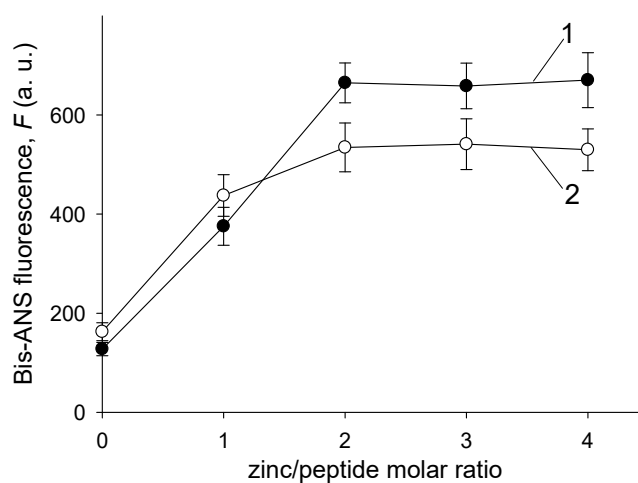


Figure 4. Dependencies of fluorescence of bis-ANS/A β complexes, F , on the Zn^{2+} /peptide molar ratio. The fluorescence was measured 30 min after the addition of Zn^{2+} . Curves 1 and 2—A β 42 and H6R-A β 42, respectively. Peptides in buffer H (10 mM HEPES, pH 6.8, 50 mM NaCl); peptide concentration—25 μ M. Bis-ANS/peptide molar ratio—1:10. The means and standard deviations for triplicate measurements are shown.

4. Discussion

The pathogenic mutations in the A β sequence, associated with the early onset of AD, are responsible for only a small percentage of all AD cases. Nonetheless, these mutations, alongside with artificial amino acid substitutions, attract a constant interest since they demonstrate a variety of A β aggregation pathways in vitro [40,41], thus allowing a better understanding of molecular mechanisms underlying the pathological A β aggregation [42]. It is well established that the English familiar mutation, H6R, promotes the self-oligomerization and fibrillar aggregation of the full-length A β peptides [30,31]. Our study elucidates the pathological role of H6R mutation in the Zn^{2+} -triggered aggregation of these peptides.

The present experimental results demonstrate that the H6R mutation in A β 42 peptides, while not suppressing the Zn^{2+} -triggered aggregation under molar excess of Zn^{2+} , as the H13A and H14A substitutions did [16], can still markedly alter the character of Zn^{2+} -induced amorphous aggregates. The approximately twice higher turbidity of H6R-A β 42 preparations at the Zn^{2+} /peptide ratios of 2 and above, compared with that for A β 42 preparations (Figure 1), altogether with the similar aggregate characteristic size (Figure 2) and degree of aggregation, suggests that optical properties (most probably, the refractive index) of formed amorphous aggregates as scattering centers are quite different. Since the aggregates are amorphous and, therefore, lack a clearly defined structural organization, this difference may reflect a variation in a density of peptide random packing. Apparently, the dissimilar structural organization of individual A β peptides in these aggregates, revealed by CD spectroscopy (Figure 3), determines the dissimilar peptide packing. It seems fair to suggest that different modes of Zn^{2+} /A β complexing govern the formation of distinct Zn^{2+} -induced aggregates in the case of A β 42 or H6R-A β 42 peptides.

The effects of H6R substitution on the Zn^{2+} /A β complexing were thoroughly studied using the A β 16 peptide as a convenient model of A β MBD [43–45]. In the intact A β 16, a monomeric complex is formed through the chelation of a zinc ion by histidine residues H6, H13, and H14 and glutamic acid residue E11 [43]. In addition, H6 can be involved in an inter-peptide coordination of zinc ions by the pairs H6/H13 and/or H14/E11 of two peptide molecules, which suggests a Zn^{2+} -bridging mechanism of A β oligomerization [45]. The exclusion of the H6 residue from the zinc chelation pattern was shown

to block the Zn^{2+} -driven A β 16 oligomerization due to a formation of stable Zn^{2+} -mediated dimers via the coordination of Zn^{2+} by the $^{11}EVHH^{14}$ regions of two H6R-A β 16 peptides [44,45]. However, in the case of full-length peptides, H6R mutation did not preclude their Zn^{2+} -induced aggregation (Figures 1 and 2). It is most likely that the lack of histidine residue H6 due to H6R substitution is compensated for by another amino acid residue of A β MBD. Indeed, amino acid residues such as D1, E3, and D7 are potentially capable of taking a part in coordinating Zn^{2+} [46]. Obviously, this should result in the structuring of MBD of the mutant peptide upon Zn^{2+} binding, different from that of the intact peptide. Since the structural rearrangement of MBD, caused by Zn^{2+} binding, is known to lead to a conformational reorganization of the C-terminal region in the intact A β [47,48], the different structuring of MBD due to the lack of H6 may alter the conformational reorganization of the C-terminal domain and, consequently, the structure of amorphous aggregates.

The double substitution R5A/H6A was reported to have no effect on the Zn^{2+} -triggered “coil-to- β -sheet” conformational transition in A β 40 peptides [15]. We could find no experimental studies devoted to the impact of R5A substitution per se on either the self- or Zn^{2+} -induced A β aggregation. Nonetheless, the molecular dynamic simulation study [29] demonstrated that such substitution can alter the structural organization of both N- and C-terminal domains of A β 42. Apparently, the change in A β 42 structural organization due to the concurrent substitution R5A leads to the different response of R5A/H6A-A β 40 peptides to Zn^{2+} , compared to that of H6R-A β 42.

5. Conclusions

The English (H6R) mutation, while not preventing the Zn^{2+} -triggered aggregation of the A β 42 peptide, was found to influence the conformational alterations in the peptide, induced by its complexing with Zn^{2+} , and, consequently, the structural characteristics of Zn^{2+} -induced amorphous aggregates. The mutant peptide H6R-A β 42 showed no appreciable changes in its structure under molar excess of Zn^{2+} , in contrast to the intact A β 42 peptide which demonstrated an increase in the random coil and β -sheet content. The formed Zn^{2+} -induced amorphous aggregates of the H6R mutant appeared structurally different from those of the intact A β 42 that was manifested by their distinct optical properties. The presented findings further advance the understanding of the pathological role of H6R mutation. Furthermore, they highlight the possibility that some other amino acid residue of A β MBD may participate in the coordinating Zn^{2+} when H6 is excluded from the chelation pattern. This possibility should be taken into account in the rational design of anti-AD drugs aimed at disrupting pathogenic Zn^{2+} -A β interactions.

Author Contributions: Conceptualization, S.P.R., S.A.K., and A.A.M.; methodology, S.P.R. and V.A.M.; validation, S.P.R. and S.A.K.; formal analysis, Y.Y.K. and D.N.K.; investigation, S.A.K., D.N.K., O.I.K., and Y.Y.K.; resources, V.A.M.; writing—original draft preparation, S.P.R.; writing—review and editing, D.N.K., S.A.K., V.A.M., and A.A.M.; visualization, S.A.K. and O.I.K.; supervision, S.P.R. and S.A.K.; project administration, V.A.M.; funding acquisition, A.A.M. All authors have read and agreed to the published version of the manuscript.

Funding: This work was supported by the Russian Science Foundation grant No. 19-74-30007.

Acknowledgments: DLS experiments were performed using the equipment of the “Human Proteome” Core Facility (Institute of Biomedical Chemistry).

Conflicts of Interest: The authors declare no conflict of interest.

References

1. Penke, B.; Bogár, F.; Fulop, L. β -Amyloid and the Pathomechanisms of Alzheimer’s Disease: A Comprehensive View. *Molecules* **2017**, *22*, 1692. [[CrossRef](#)]
2. Eisele, Y.S.; Duyckaerts, C. Propagation of A β pathology: Hypotheses, discoveries, and yet unresolved questions from experimental and human brain studies. *Acta Neuropathol.* **2015**, *131*, 5–25. [[CrossRef](#)]
3. Tamagno, E.; Guglielmotto, M.; Monteleone, D.; Manassero, G.; Vasciaveo, V.; Tabaton, M. The Unexpected Role of A β 1-42 Monomers in the Pathogenesis of Alzheimer’s Disease. *J. Alzheimer’s Dis.* **2018**, *62*, 1241–1245. [[CrossRef](#)]

4. Atrián-Blasco, E.; Gonzalez, P.; Santoro, A.; Alies, B.; Faller, P.; Hureau, C. Cu and Zn coordination to amyloid peptides: From fascinating chemistry to debated pathological relevance. *Co-ord. Chem. Rev.* **2018**, *371*, 38–55. [[CrossRef](#)]
5. Wang, P.; Wang, Z.-Y. Metal ions influx is a double edged sword for the pathogenesis of Alzheimer's disease. *Ageing Res. Rev.* **2017**, *35*, 265–290. [[CrossRef](#)]
6. Bush, A.I.; Pettingell, W.; Multhaup, G.; Paradis, M.D.; Vonsattel, J.; Gusella, J.; Beyreuther, K.; Masters, C.; Tanzi, R. Rapid induction of Alzheimer A beta amyloid formation by zinc. *Science* **1994**, *265*, 1464–1467. [[CrossRef](#)]
7. Serrano-Pozo, A.; Frosch, M.P.; Masliah, E.; Hyman, B.T. Neuropathological Alterations in Alzheimer Disease. *Cold Spring Harb. Perspect. Med.* **2011**, *1*, a006189. [[CrossRef](#)] [[PubMed](#)]
8. Lovell, M.A.; Robertson, J.; Teesdale, W.J.; Campbell, J.L.; Markesbery, W.R. Copper, iron and zinc in Alzheimer's disease senile plaques. *J. Neurol. Sci.* **1998**, *158*, 47–52. [[CrossRef](#)]
9. Miller, L.; Wang, Q.; Telivala, T.P.; Smith, R.J.; Lanzirrotti, T.; Miklossy, J.; Miklossy, J. Synchrotron-based infrared and X-ray imaging shows focalized accumulation of Cu and Zn co-localized with β -amyloid deposits in Alzheimer's disease. *J. Struct. Biol.* **2006**, *155*, 30–37. [[CrossRef](#)] [[PubMed](#)]
10. Faller, P.; Hureau, C.; Berthoumieu, O. Role of Metal Ions in the Self-assembly of the Alzheimer's Amyloid- β Peptide. *Inorg. Chem.* **2013**, *52*, 12193–12206. [[CrossRef](#)] [[PubMed](#)]
11. Lee, J.-Y.; Cole, T.B.; Palmiter, R.D.; Suh, S.W.; Koh, J.-Y. Contribution by synaptic zinc to the gender-disparate plaque formation in human Swedish mutant APP transgenic mice. *Proc. Natl. Acad. Sci. USA* **2002**, *99*, 7705–7710. [[CrossRef](#)] [[PubMed](#)]
12. Adlard, P.A.; Bush, I.A. Metals and Alzheimer's Disease: How Far Have We Come in the Clinic? *J. Alzheimer's Dis.* **2018**, *62*, 1369–1379. [[CrossRef](#)] [[PubMed](#)]
13. Kulikova, A.A.; Makarov, A.A.; Kozin, S.A. Roles of zinc ions and structural polymorphism of β -amyloid in the development of Alzheimer's disease. *Mol. Biol.* **2015**, *49*, 217–230. [[CrossRef](#)]
14. Liu, S.-T.; Howlett, G.; Barrow, C.J. Histidine-13 Is a Crucial Residue in the Zinc Ion-Induced Aggregation of the A β Peptide of Alzheimer's Disease. *Biochemistry* **1999**, *38*, 9373–9378. [[CrossRef](#)] [[PubMed](#)]
15. Yang, D.S.; McLaurin, J.; Qin, K.; Westaway, D.; Fraser, P.E. Examining the zinc binding site of the amyloid- β peptide. *J. Biol. Inorg. Chem.* **2000**, *267*, 6692–6698. [[CrossRef](#)] [[PubMed](#)]
16. Tôugu, V.; Karafin, A.; Zovo, K.; Chung, R.; Howells, C.; West, A.K.; Palumaa, P. Zn(II)- and Cu(II)-induced non-fibrillar aggregates of amyloid- β (1-42) peptide are transformed to amyloid fibrils, both spontaneously and under the influence of metal chelators. *J. Neurochem.* **2009**, *110*, 1784–1795. [[CrossRef](#)]
17. Janssen, J.; Beck, J.; Campbell, T.; Dickinson, A.; Fox, N.; Harvey, R.; Houlden, H.; Rossor, M.; Collinge, J. Early onset familial Alzheimer's disease: Mutation frequency in 31 families. *Neurology* **2003**, *60*, 235–239. [[CrossRef](#)]
18. Khmeleva, S.; Radko, S.; Kozin, S.A.; Kiseleva, Y.Y.; Mezentsev, Y.V.; Mitkevich, V.A.; Kurbatov, L.K.; Ivanov, A.; Makarov, A.A. Zinc-Mediated Binding of Nucleic Acids to Amyloid- β Aggregates: Role of Histidine Residues. *J. Alzheimer's Dis.* **2016**, *54*, 809–819. [[CrossRef](#)]
19. Radko, S.; Khmeleva, S.A.; Kiseleva, Y.Y.; Kozin, S.A.; Mitkevich, V.A.; Makarov, A.A. Effects of the H6R and D7H Mutations on the Heparin-Dependent Modulation of Zinc-Induced Aggregation of Amyloid β . *Mol. Biol.* **2019**, *53*, 922–928. [[CrossRef](#)]
20. Jan, A.; Hartley, D.M.; A Lashuel, H. Preparation and characterization of toxic A β aggregates for structural and functional studies in Alzheimer's disease research. *Nat. Protoc.* **2010**, *5*, 1186–1209. [[CrossRef](#)]
21. Böhm, G.; Muhr, R.; Jaenicke, R. Quantitative analysis of protein far UV circular dichroism spectra by neural networks. *Protein Eng. Des. Sel.* **1992**, *5*, 191–195. [[CrossRef](#)] [[PubMed](#)]
22. Greenfield, N.J. Using circular dichroism spectra to estimate protein secondary structure. *Nat. Protoc.* **2006**, *1*, 2876–2890. [[CrossRef](#)] [[PubMed](#)]
23. Suprun, E.V.; Khmeleva, S.; Kiseleva, Y.Y.; Radko, S.P.; Archakov, A.I.; Shumyantseva, V. Quantitative Aspects of Electrochemical Detection of Amyloid- β Aggregation. *Electroanalysis* **2016**, *28*, 1977–1983. [[CrossRef](#)]
24. Bitan, G.; Kirkitadze, M.D.; Lomakin, A.; Vollers, S.S.; Benedek, G.B.; Teplow, D.B. Amyloid β -protein (A β) assembly: A β 40 and A β 42 oligomerize through distinct pathways. *Proc. Natl. Acad. Sci. USA* **2002**, *100*, 330–335. [[CrossRef](#)] [[PubMed](#)]
25. Bartolini, M.; Bertucci, C.; Cavrini, V.; Andrisano, V. β -Amyloid aggregation induced by human acetylcholinesterase: Inhibition studies. *Biochem. Pharmacol.* **2003**, *65*, 407–416. [[CrossRef](#)]

26. Bartolini, M.; Bertucci, C.; Bolognesi, M.L.; Cavalli, A.; Melchiorre, C.; Andrisano, V. Insight Into the Kinetic of Amyloid β (1–42) Peptide Self-Aggregation: Elucidation of Inhibitors' Mechanism of Action. *ChemBioChem* **2007**, *8*, 2152–2161. [[CrossRef](#)]
27. Xu, L.; Chen, Y.; Wang, X. Dual effects of familial Alzheimer's disease mutations (D7H, D7N, and H6R) on amyloid β peptide: Correlation dynamics and zinc binding. *Proteins: Struct. Funct. Bioinform.* **2014**, *82*, 3286–3297. [[CrossRef](#)]
28. Yang, M.; Teplow, D.B. Amyloid β -Protein Monomer Folding: Free-Energy Surfaces Reveal Alloform-Specific Differences. *J. Mol. Biol.* **2008**, *384*, 450–464. [[CrossRef](#)]
29. Coskuner-Weber, O.; Uversky, V.N. Insights into the Molecular Mechanisms of Alzheimer's and Parkinson's Diseases with Molecular Simulations: Understanding the Roles of Artificial and Pathological Missense Mutations in Intrinsically Disordered Proteins Related to Pathology. *Int. J. Mol. Sci.* **2018**, *19*, 336. [[CrossRef](#)]
30. Hori, Y.; Hashimoto, T.; Wakutani, Y.; Urakami, K.; Nakashima, K.; Condrón, M.M.; Tsubuki, S.; Saido, T.C.; Teplow, D.B.; Iwatsubo, T. The Tottori (D7N) and English (H6R) Familial Alzheimer Disease Mutations Accelerate A β Fibril Formation without Increasing Protofibril Formation. *J. Biol. Chem.* **2006**, *282*, 4916–4923. [[CrossRef](#)]
31. Ono, K.; Condrón, M.M.; Teplow, D.B. Effects of the English (H6R) and Tottori (D7N) Familial Alzheimer Disease Mutations on Amyloid β -Protein Assembly and Toxicity. *J. Biol. Chem.* **2010**, *285*, 23186–23197. [[CrossRef](#)] [[PubMed](#)]
32. Banerjee, R. Effect of Curcumin on the metal ion induced fibrillization of Amyloid- β peptide. *Spectrochim. Acta Part A: Mol. Biomol. Spectrosc.* **2014**, *117*, 798–800. [[CrossRef](#)] [[PubMed](#)]
33. Zhang, T.; Pauly, T.; Nagel-Steger, L. Stoichiometric Zn²⁺ interferes with the self-association of A β 42: Insights from size distribution analysis. *Int. J. Biol. Macromol.* **2018**, *113*, 631–639. [[CrossRef](#)] [[PubMed](#)]
34. Janaszewska, A.; Klajnert-Maculewicz, B.; Marcinkowska, M.; Duchnowicz, P.; Appelhans, D.; Grasso, G.; Deriu, M.; Danani, A.; Cangiotti, M.; Ottaviani, M.F. Multivalent interacting glycodendrimer to prevent amyloid-peptide fibril formation induced by Cu(II): A multidisciplinary approach. *Nano Res.* **2018**, *11*, 1204–1226. [[CrossRef](#)]
35. Radko, S.P.; Khmeleva, S.; Suprun, E.V.; Kozin, S.A.; Bodoev, N.V.; Makarov, A.A.; Archakov, A.I.; Shumyantseva, V.V. Physico-chemical methods for studying amyloid- β aggregation. *Biochem. (Moscow) Suppl. Ser. B Biomed. Chem.* **2015**, *9*, 258–274. [[CrossRef](#)]
36. Hawe, A.; Sutter, M.; Jiskoot, W. Extrinsic Fluorescent Dyes as Tools for Protein Characterization. *Pharm. Res.* **2008**, *25*, 1487–1499. [[CrossRef](#)]
37. Chen, W.-T.; Liao, Y.-H.; Yu, H.-M.; Cheng, I.H.; Chen, Y.-R. Distinct Effects of Zn²⁺, Cu²⁺, Fe³⁺, and Al³⁺ on Amyloid- β Stability, Oligomerization, and Aggregation. *J. Biol. Chem.* **2011**, *286*, 9646–9656. [[CrossRef](#)]
38. Chen, W.-T.; Hong, C.-J.; Lin, Y.-T.; Chang, W.-H.; Huang, H.-T.; Liao, J.-Y.; Chang, Y.-J.; Hsieh, Y.-F.; Cheng, C.-Y.; Liu, H.-C.; et al. Amyloid-Beta (A β) D7H Mutation Increases Oligomeric A β 42 and Alters Properties of A β -Zinc/Copper Assemblies. *PLOS ONE* **2012**, *7*, e35807. [[CrossRef](#)]
39. Radko, S.P.; Khmeleva, S.; Mantsyzov, A.B.; Kiseleva, Y.Y.; Mitkevich, V.A.; Kozin, S.A.; Makarov, A.A. Heparin Modulates the Kinetics of Zinc-Induced Aggregation of Amyloid- β Peptides. *J. Alzheimer's Dis.* **2018**, *63*, 539–550. [[CrossRef](#)]
40. Hatami, A.; Monjazeb, S.; Milton, S.; Glabe, C.G. Familial Alzheimer's Disease Mutations within the Amyloid Precursor Protein Alter the Aggregation and Conformation of the Amyloid- β Peptide. *J. Biol. Chem.* **2017**, *292*, 3172–3185. [[CrossRef](#)]
41. Grasso, G.; Leanza, L.; Morbiducci, U.; Danani, A.; Deriu, M.A. Aminoacid substitutions in the glycine zipper affect the conformational stability of amyloid beta fibrils. *J. Biomol. Struct. Dyn.* **2019**, 1–8. [[CrossRef](#)] [[PubMed](#)]
42. Chiti, F.; Stefani, M.; Taddei, N.; Ramponi, G.; Dobson, C.M. Rationalization of the effects of mutations on peptide and protein aggregation rates. *Nature* **2003**, *424*, 805–808. [[CrossRef](#)] [[PubMed](#)]
43. Tsvetkov, P.O.; Kulikova, A.A.; Golovin, A.V.; Tkachev, Y.V.; Archakov, A.I.; Kozin, S.A.; Makarov, A.A. Minimal Zn²⁺ Binding Site of Amyloid- β . *Biophys. J.* **2010**, *99*, L84–L86. [[CrossRef](#)]
44. Kozin, S.A.; Kulikova, A.A.; Istrate, A.; Tsvetkov, P.O.; Zhokhov, S.; Mezentsev, Y.V.; Kechko, O.I.; Ivanov, A.; Polshakov, V.; Makarov, A.A. The English (H6R) familial Alzheimer's disease mutation facilitates zinc-induced dimerization of the amyloid- β metal-binding domain. *Metallomics* **2015**, *7*, 422–425. [[CrossRef](#)] [[PubMed](#)]

45. Istrate, A.; Kozin, S.A.; Zhokhov, S.S.; Mantsyzov, A.B.; Kechko, O.I.; Pastore, A.; Makarov, A.A.; Polshakov, V. Interplay of histidine residues of the Alzheimer's disease A β peptide governs its Zn-induced oligomerization. *Sci. Rep.* **2016**, *6*, 21734. [[CrossRef](#)] [[PubMed](#)]
46. Miller, Y.; Ma, B.; Nussinov, R. Metal binding sites in amyloid oligomers: Complexes and mechanisms. *Co-ord. Chem. Rev.* **2012**, *256*, 2245–2252. [[CrossRef](#)]
47. Lim, K.H.; Kim, Y.K.; Chang, Y.-T. Investigations of the Molecular Mechanism of Metal-Induced A β (1–40) Amyloidogenesis†. *Biochemistry* **2007**, *46*, 13523–13532. [[CrossRef](#)]
48. Olofsson, A.; Lindhagen-Persson, M.; Vestling, M.; Sauer-Eriksson, A.E.; Öhman, A. Quenched hydrogen/deuterium exchange NMR characterization of amyloid- β peptide aggregates formed in the presence of Cu²⁺ or Zn²⁺. *FEBS J.* **2009**, *276*, 4051–4060. [[CrossRef](#)]



© 2020 by the authors. Licensee MDPI, Basel, Switzerland. This article is an open access article distributed under the terms and conditions of the Creative Commons Attribution (CC BY) license (<http://creativecommons.org/licenses/by/4.0/>).